Energy partition in kinetic turbulence in strongly magnetized plasmas

L.M. Fazendeiro[1], N.F. Loureiro[1]

[1] *Instituto de Plasmas e Fusão Nuclear, IST, Universidade de Lisboa, 1049-001 Lisboa, Portugal*

Introduction: Turbulence is one of the fundamental unsolved problems in classical physics, ubiquitous in both laboratory and astrophysical plasmas [1]. In many cases of interest (e.g., the solar corona, the interstellar medium or the core of modern-day tokamaks) the collisional frequency is so small compared to the dynamic frequencies of interest that a fluid approach is not justified and a kinetic description is thus required. Due to the huge computational costs involved in performing fully kinetic ($6D$) simulations of turbulent plasmas, there is great advantage in utilizing reduced models that can still accurately capture the main relevant aspects of the problem. In addition, our physical understanding may also be greatly enhanced by them. One such fluid-kinetic model is KREHM (Kinetic Reduced Electron Heating Model), a rigorous asymptotic reduction of gyrokinetics in the limit of electron plasma beta $\beta_e \sim m_e/m_i$ [2]. The model has been numerically implemented in the `Viriato` code [3, 4], used in this work, in which we simulate decaying kinetic Alfvénic turbulence in $3D$, starting from an Orszag-Tang (OT) initial condition [5].

Model and code benchmarks: In KREHM the perturbed electron distribution function is defined as $\delta f_e = g_e + (\delta n_e/n_{0e} + 2v_\parallel u_{\parallel e}/v_{the}^2)F_{0e}$, where F_{0e} is the equilibrium Maxwellian, $v_{\text{the}} = \sqrt{2T_{0e}/m_e}$ the electron thermal speed, $v_\parallel$ the velocity coordinate (parallel to the magnetic guide field, B_0), δn_e is the electron density perturbation (the zeroth moment of δf_e), $u_{\parallel e} = (e/cm_e)d_e^2\nabla_\perp^2 A_\parallel$ is the parallel electron flow (the first moment of δf_e), $A_\parallel$ is the parallel component of the vector potential, and $d_e = c/\omega_{pe}$ is the electron skin depth, with $\omega_{pe} = \sqrt{4\pi ne^2/m_e}$ the electron plasma frequency. The KREHM equations are [2]:

$$\frac{1}{n_{0e}}\frac{d\delta n_e}{dt} = -\hat{\boldsymbol{b}}\cdot\nabla\frac{e}{cm_e}d_e^2\nabla_\perp^2 A_\parallel, \tag{1}$$

$$\frac{d}{dt}\left(A_\parallel - d_e^2\nabla_\perp^2 A_\parallel\right) = \eta\nabla_\perp^2 A_\parallel - c\frac{\partial\varphi}{\partial z} + \frac{cT_{0e}}{e}\hat{\boldsymbol{b}}\cdot\nabla\left(\frac{\delta n_e}{n_{0e}} + \frac{\delta T_{\parallel e}}{T_{0e}}\right), \tag{2}$$

$$\frac{dg_e}{dt} + v_\parallel\hat{\boldsymbol{b}}\cdot\nabla\left(g_e - \frac{\delta T_{\parallel e}}{T_{0e}}F_{0e}\right) = C[g_e] + \left(1 - \frac{2v_\parallel^2}{v_{\text{the}}^2}\right)F_{0e}\hat{\boldsymbol{b}}\cdot\nabla\frac{e}{cm_e}d_e^2\nabla_\perp^2 A_\parallel, \tag{3}$$

where $\frac{d}{dt} = \frac{\partial}{\partial t} + \frac{c}{B_0}[\varphi,\ldots]$, $\hat{\boldsymbol{b}}\cdot\nabla = \frac{\partial}{\partial z} - \frac{1}{B_0}\left[A_\parallel,\ldots\right]$ and $[\ldots,\ldots]$ denotes the Poisson bracket. $C[g_e]$ is the collision operator and η the Ohmic resistivity. The electrostatic potential, φ, is given by the gyrokinetic Poisson law $\frac{\delta n_e}{n_{0e}} = \frac{Z}{\tau}\left(\hat{\Gamma}_0 - 1\right)\frac{e\varphi}{T_{0e}}$, with $\tau = T_{0i}/T_{0e}$ and $\hat{\Gamma}_0$ denoting the inverse Fourier transform of $\Gamma_0(\alpha) = I_0(\alpha)e^{-\alpha}$; I_0 is the modified Bessel function and $\alpha = k_\perp^2\rho_i^2/2$, with ρ_i the ion Larmor radius. Equation (3) is a kinetic equation for the reduced electron distribution function $g_e(x,y,z,v_\parallel,v_\perp,t)$, with no explicit dependence on $v_\perp$. If such a dependence is not introduced by the collision operator $C[g_e]$ [2], then $v_\perp$ can be integrated out and g_e effectively becomes only $4D$, $g_e(x,y,z,v_\parallel)$. In `Viriato` g_e is expanded in Hermite polynomials, which transforms the electron drift-kinetic eq. (3), into a coupled set of M

fluid-like equations for each of the coefficients (g_m) of the Hermite polynomials of order m [2].

In Fig. 1 we show two of the many benchmarks performed with `Viriato` [4]. The left plot is a direct comparison with the gyrokinetic code `AstroGK` [6], where the linear growth rate of the tearing mode is computed for several values of the Lundquist number, $S = av_A/\eta$, where a is a typical equilibium length scale and $v_A = B_0/\sqrt{4\pi n_0 m_i}$ the Alfvén speed based on the guide-field. The parallel Alfvén time is defined as $\tau_A = L_\parallel/v_A$, where $L_\parallel$ is the reference length-scale, parallel to the guide field. We note that for $\beta_e \sim 30 m_e/m_i$ the agreement is already quite good, suggesting that KREHM may well be a valid description of plasma dynamics outside its strict asymptotic limit of validity. The right plot shows a calculation of the frequency and damping rate of the kinetic Alfvén wave (KAW), whose dispersion relation can be obtained by linearizing eqs. (1–3), showing an excellent agreement between the analytical prediction and the numerical results obtained with `Viriato`.

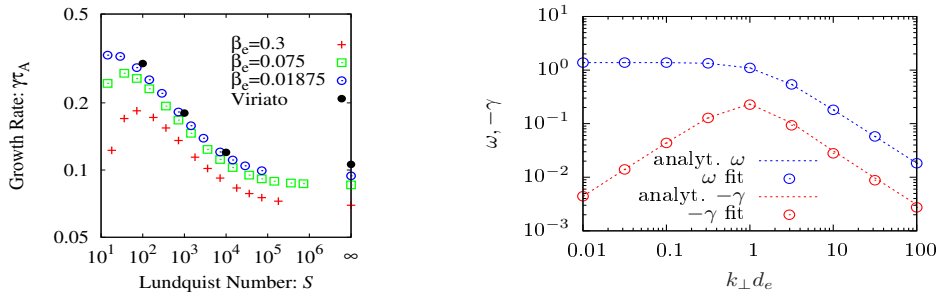

Figure 1: Left: Tearing mode growth rate as a function of the Lundquist number; results obtained both with the gyrokinetic code `AstroGK` [6], for varying values of β_e, and `Viriato`. Right: Frequency and damping rate of the linear kinetic Alfvén wave (KAW), in units of τ_A, at fixed $k_\perp \rho_i = 1$, $M = 20$, as a function of d_e. Lines are the exact solution of the analytical dispersion relation, data points were obtained with `Viriato`.

Main results and discussion: In this work, the KREHM equations are solved in a $3D$ periodic cubic box of size 2π in each direction and 256^3 points. In these simulations there are two available channels for energy dissipation: one via hyperdiffusion in coordinate space ($k-$space in `Viriato`) and the other (if non-isothermal electrons, and thus $g_e \neq 0$ are considered) via hypercollisions in the $m-$space of the Hermite polynomials. Thus, and similar to the energy cascade occurring from small k (where energy is injected) to large k (where dissipation takes over), in the familiar Richardson picture, there is now also transfer of energy occurring from small to large m, i.e., phase-mixing in velocity space.

In Fig. 2 we show two energy spectra for the case of decaying $3D$ OT kinetic turbulence, with parameters $\rho_i = 2$, $d_e = 0.3$ (in code units) and non-isothermal electrons, with $M = 40$ Hermite polynomials, at two different times. The slopes indicated refer to power laws that have been widely discussed in the literature. In particular, we see that there is a sharp separation between electric and magnetic energy scalings, occurring at around $(k_\perp/2\pi)\rho_i \sim 1$, in agreement with solar wind observations [7]. Also shown is a -2.8 slope often reported in observations of the solar wind (e.g., [8]).

In Fig. 3 we show the result of the competition between the two energy dissipation channels, for

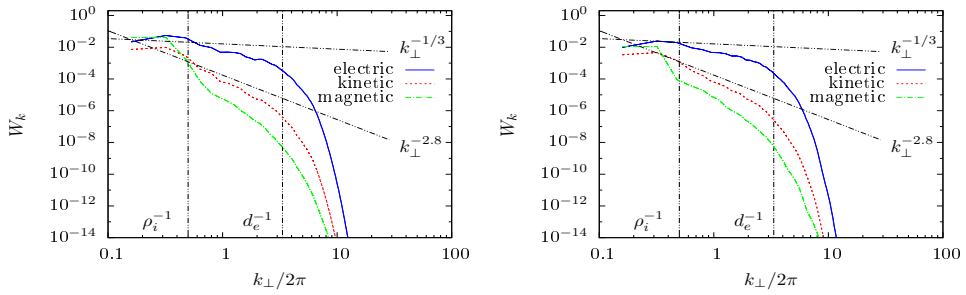

Figure 2: Spectra for decaying turbulence with $\rho_i = 2$, $d_e = 0.3$ and $M = 40$ at $t/\tau_A = 1.5$ (left) and 3.0 (right). Blue line represents perpendicular electric energy; red line kinetic energy, green the perpendicular magnetic field energy. See text for discussion of the power laws.

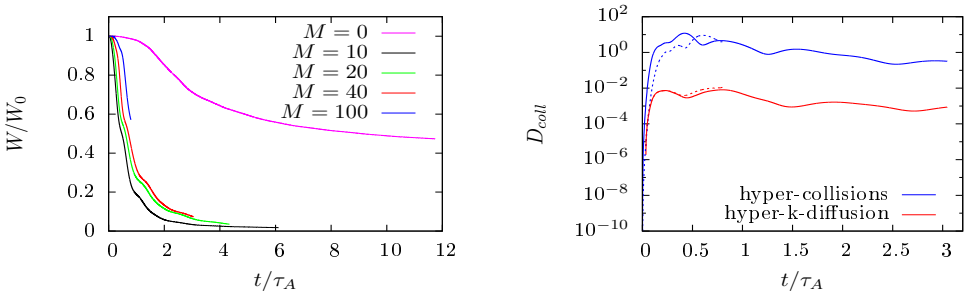

Figure 3: Left: Total energy, normalized to its initial value, W_0, for a 256^3 system, with $\rho_i = 2$, $d_e = 0.3$. Note the dramatic decrease in energy decay rate when the $m's$ are switched off ($M = 0$). Right: Energy dissipation channels for the $M = 40$ (full lines) and $M = 100$ (dotted lines) runs. The predominance of the hyper-collisions (in m space) in both cases is clearly displayed.

the same parameters of Fig. 2. The left plot shows the values of total energy, normalized to its initial value, for a case with isothermal electrons ($M = 0$, i.e., $g_e = 0$) and for a successively higher number of Hermite polynomials. The different durations of the runs are due to the fact that they become much more computationally expensive as M increases. The right plot shows the total values for each of the two dissipation channels: hyperdiffusion in $k-$space and hypercollisions, corresponding to the energy cascade in velocity space (linear phase-mixing). This is shown for two runs only ($M = 40, 100$) but the $M = 10, 20$ runs also display the same behaviour. Note also that the run with $M = 100$ (dotted lines) takes longer to reach the same value of energy dissipation via hyper-collisions, in accordance with its slower energy decay rate, shown in the left plot.

Finally, for completeness, we show in Fig. 4 (left) energy spectra in $m-$space for this set of runs, at $t = 0.73\tau_A$. This plot clearly illustrates how the inertial range develops as the number of Hermite polynomials increases and the system subsequentely takes longer to reach the dissipation range. Also shown is a $-1/2$ power law, deduced in [2] for the inertial range slope of linear phase-mixing KAWs. The right plot shows energy spectra for $M = 40$ at the same times as Fig. 2. The power law seems to be obeyed, well beyond its regime of validity, even after most of the initial energy has been dissipated.

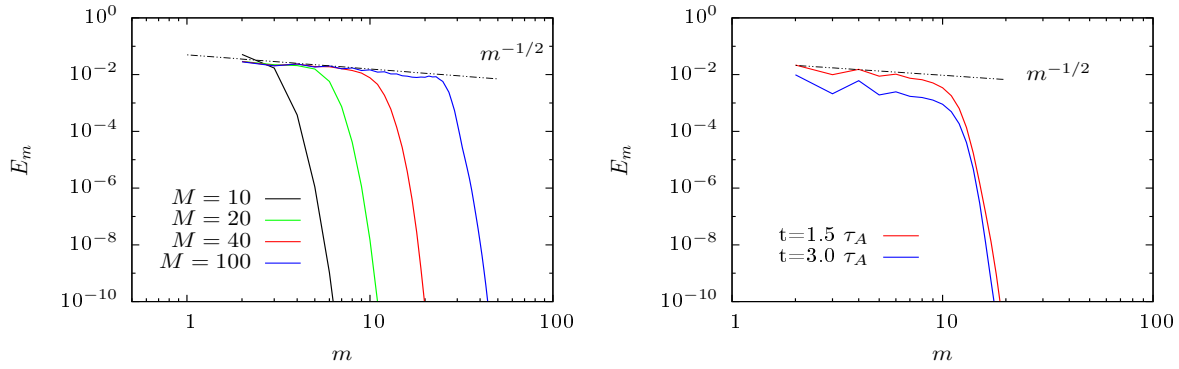

Figure 4: $E_m = |g_m^2|/2$ energy spectra in $m-$space, with a $-1/2$ power law [2]. Left: same values of $M \neq 0$ shown in Fig. 3 (left), at the same time, $t = 0.73\tau_A$. Right: Spectra for the $M = 40$ run, at two different times, the same as shown in Fig. 2.

Conclusions and future work: In this work we show preliminary results suggesting that linear phase-mixing may play a dominant role in decaying kinetic turbulence energy dissipation. We note that these results are still not conclusive and further parameter scans are in progress. In particular, the non-linearity of the system only becomes effective at about $t \sim \tau_A$ (see Fig. 3, left, $M = 0$ run). This means that for non-isothermal electrons ($g_e \neq 0$, i.e., $M \neq 0$) linear phase-mixing begins dissipating energy well before the other channel (in k-space) can do so. However, there is a strong indication (from the results presented here as well as from other, smaller runs) that this may indeed be the dominant energy dissipation mechanism in these systems, a topic which will be the main subject of a forthcoming publication.

Other questions of interest include ascertaining the exact role played by current sheets in energy dissipation [9, 10]. In order to quantify this we intend to perform numerical simulations where turbulent mixing (due to nonlinearity) and linear phase-mixing in velocity space are taking place simultaneously, which in turn will require increasing the number of Hermite polynomials even further.

Acknowledgements: This work was partly supported by Fundação para a Ciência e Tecnologia via Grants UID/FIS/50010/2013 and IF/00530/2013. Simulations were carried out at Helios (IFERC) and Stampede (TACC).

References

[1] A.A. Schekochihin, S.C. Cowley, W. Dorland *et al*, Astrophys. J. Suppl. S., **182**, 310-377 (2009).

[2] A. Zocco and A.A. Schekochihin, Phys. Plasmas, **18**, 2309 (2011).

[3] N.F. Loureiro, A.A. Schekochihin and A. Zocco, Phys. Rev. Lett. **111**, 025002 (2013).

[4] N.F. Loureiro, W. Dorland, L.M. Fazendeiro *et al.*, arXiv:1505.02649, submitted to J. Comput. Phys., (2015).

[5] S.A. Orszag and C.-M. Tang, J. Fluid Mech., **90**, 01, (1979).

[6] R. Numata, G.G. Howes, T. Tatsuno *et al.*, J. Comp. Phys., **229**, 24, (2010).

[7] S. Bale, P. Kellogg, F. Mozer *et al.*, Phys. Rev. Lett., **94**, 21, (2005).

[8] O. Alexandrova, J. Saut, C. Lacombe *et al.*, Phys. Rev. Lett., **103**, 16, (2009).

[9] V. Zhdankin, D.A. Uzdensky and S. Boldyrev, Phys. Rev. Lett., **114**, 065002, (2015).

[10] K.D. Makwana, V. Zhdankin, H. Li *et al.*, Phys. Plasmas, **22**, 042902, (2015).